



# Emmetropes and myopes differ little in their accommodation dynamics but strongly in their ciliary muscle morphology

Sandra Wagner<sup>a,\*</sup>, Eberhart Zrenner<sup>a,b</sup>, Torsten Strasser<sup>a</sup>

<sup>a</sup> Institute for Ophthalmic Research, Eberhard Karls University Tuebingen, Elfriede-Aulhorn-Str. 7, 72076 Tuebingen, Germany

<sup>b</sup> Werner Reichardt Centre for Integrative Neuroscience (CIN) Tuebingen, Otfried-Mueller-Str. 25, 72076 Tuebingen, Germany

## ARTICLE INFO

### Keywords:

Ciliary muscle  
Accommodation  
Myopia  
Optical coherence tomography  
Near vision

## ABSTRACT

Previous work suggested an association between near vision and myopia. We therefore investigated the accommodation process in emmetropes and myopes regarding morphologic changes of the ciliary muscle (CM) and power changes of the lens for different accommodation demands. The temporal CM of 18 emmetropic and 20 myopic students was imaged via anterior segment optical coherence tomography during far and near accommodation (2.5D, 3D, 4D). Additionally, accommodation dynamics to the stimuli pattern far-near-far (15 s each; 2.5D, 3D, 4D) were recorded with eccentric infrared photorefraction. OCT images were processed using custom-developed software facilitating the analysis of selective CM thickness (CMT) readings and CMT profiles. Anterior CMT readings were significantly smaller in myopes. Starting at 1.4 mm posterior to the scleral spur (SP), myopic CM became thicker than emmetropic. Anterior CMT changes ( $\Delta$ CMT) continuously increased with accommodation demand in myopes while emmetropic  $\Delta$ CMT only increased from 2.5D to 3D. Compared to emmetropes, myopes showed smaller  $\Delta$ CMT but increased CM movement relative to SP. There were no significant differences between the groups for accommodation changes from far to near vision and vice versa, velocity, microfluctuations, power spectra or lag of accommodation. At 4 D, larger  $\Delta$ CMT were associated with lower lens changes for disaccommodation. While CM shape, movement, and thickness showed distinct differences depending on refractive error, emmetropes and myopes did not differ in their dynamic accommodation. Further analysis is necessary to evaluate whether the CM's anatomical shape or predispositions in its intramuscular constituents are causative factors in myopigenesis.

## 1. Introduction

In view of a predicted increase of highly myopic people worldwide (Holden et al., 2016), the vision research community is strained under the weight of understanding the development of myopia in the first place and finding treatment strategies to slow myopia progression to prevent it from reaching the vision-threatening high degrees. Several hypotheses for the elongation of the eye and thereby myopia onset have been proposed, many of them being supported by animal and human studies. One hypothesis of myopigenesis is focused on the relationship between myopia and near vision. Previous studies provided evidence for myopia prevalence being associated with the degree of education and the amount of nearwork (Morgan & Rose, 2013; Verhoeven et al., 2013; Williams et al., 2015). Moreover, the accommodation of myopes was found to show larger microfluctuations (Day, Strang, Seidel, Gray, & Mallen, 2006; Harb, Thorn, & Troilo, 2006), increased under-accommodation, the so-called lag of accommodation (Gwiazda, Thorn,

Bauer, & Held, 1993; McBrien & Millodot, 1986; Nakatsuka, Hasebe, Nonaka, & Ohtsuki, 2005; Tarrant, Severson, & Wildsoet, 2008), and a lower resting state (Maddock, Millodot, Leat, & Johnson, 1981; McBrien & Millodot, 1987) compared to their emmetropic counterparts. These characteristics, providing or contributing to a hyperopic retinal defocus, are thought to trigger the axial growth of the eye. Further investigations revealed that myopes, compared to emmetropes, have a higher susceptibility to nearwork-induced transient myopia (Ciuffreda & Vasudevan, 2008; Ciuffreda & Wallis, 1998).

The mechanism of accommodation is initiated by the action of the ciliary muscle whose contraction leads to a shape change of the crystalline lens and thereby to an increase of refractive power. Optical coherence tomography (OCT), ultrasound biomicroscopy (UBM), and magnet resonance imaging (MRI) have previously been applied to study the ciliary muscle's morphology during accommodation in different subject groups. Maximum, proportional or selective readings of the ciliary muscle thickness (CMT) or area measurements have been taken.

\* Corresponding author.

E-mail address: [sandra.wagner@uni-tuebingen.de](mailto:sandra.wagner@uni-tuebingen.de) (S. Wagner).

<https://doi.org/10.1016/j.visres.2019.08.002>

Received 24 May 2019; Received in revised form 23 July 2019; Accepted 5 August 2019

Available online 28 August 2019

0042-6989/ © 2019 Elsevier Ltd. All rights reserved.

Few trials were dedicated to comparing the muscle morphology in myopic vs. non-myopic participants: Bailey and colleagues observed a statistically significant univariate correlation between axial length and CMT at 2 and 3 mm distance from the scleral spur in a group of children between 8 and 15 years (Bailey, Sinnott, & Mutti, 2008). Analyzing the ciliary muscle changes in 32 non-myopic and 30 myopic subjects between 18 and 40 years, Buckhurst et al. found a significant association between the mean spherical error and CMT, whereby the ciliary muscle was significantly thicker at 2 and 3 mm posterior to the scleral spur in myopic compared to emmetropic eyes (Buckhurst, Gilmartin, Cubbidge, Nagra, & Logan, 2013). A trial with 269 children resulted in the same outcome for the posterior ciliary muscle and additionally revealed that a thicker apical ciliary muscle is associated with higher degrees of hyperopia (Pucker, Sinnott, Kao, & Bailey, 2013). Using UBM, Muftuoglu and colleagues measured significantly larger CMT values in eyes with unilateral high myopia than in the normal fellow eyes (Muftuoglu, Hosal, & Zilelioglu, 2009). Region-specific differences in the ciliary muscles of anisometropic subjects were observed by Kuchem et al., with more myopic eyes exhibiting thicker ciliary muscles in the longitudinal fiber portion and contrarily thinner muscles in the apical region (Kuchem, Sinnott, Kao, & Bailey, 2013). It has been suggested that a thicker ciliary muscle might prevent the equatorial stretch needed to maintain emmetropia, thereby being a factor in myopigenesis (Mutti, 2010). However, Sheppard and Davies have found a correlation between axial length and ciliary muscle length, but not between axial length and CMT when investigating the muscle morphology in fifty 19- to 34-year old subjects (Sheppard & Davies, 2010). Furthermore, proportional or selective thickness readings of the ciliary muscle have been taken while providing various accommodation demands (Jeon, Lee, Lee, & Moon, 2012; Lossing, Sinnott, Richdale, & Bailey, 2012; Richdale et al., 2012; Ruggeri et al., 2016; Shao et al., 2013; Sheppard & Davies, 2010), and the results led to suggestions of a linear relationship between CMT changes and accommodation response (Lewis, Kao, Sinnott, & Bailey, 2012; Richdale et al., 2013).

The purpose of the current investigation was to analyze and compare the morphologic changes across the entire ciliary muscle boundary in emmetropic and myopic young adults for different accommodation demands using a newly developed semi-automatic analysis tool for OCT images, and to correlate these measurements with the accommodation dynamics.

## 2. Material and methods

### 2.1. Subjects

18 emmetropic (5 males; age  $22.1 \pm 2.1$  years) and 20 myopic students (4 males; age  $22.0 \pm 1.7$  years) of the University of Tuebingen, Germany, participated in the study. Prior to the measurements, the volunteers were informed about the aims, procedures, and possible risks of the trial and only participated after having given written informed consent. The study adhered to the tenets of the Declaration of Helsinki and was approved by the Institutional Review Board of the medical faculty of the University of Tuebingen.

### 2.2. Measurement procedure

An initial visit was arranged to perform the anamnesis and pre-measurements. Subsequent to an objective refraction (ZEISS *i.Profiler<sup>plus</sup>*, Carl Zeiss Vision GmbH, Aalen, Germany), a subjective refraction obeying the rule of least negative correction for maximum achievable visual acuity (VA) was undertaken using a digital phoropter (ZEISS *Visuphor 500*, Carl Zeiss Vision GmbH, Aalen, Germany). The astigmatic refractive error was limited to  $\leq 0.75$  D. Subjects with spherical equivalent refractive errors in the range of  $\pm 0.50$  D were assigned to the emmetropic group. Both monocular and binocular VA was tested, and in myopic subjects, all being regular soft contact lens

wearers, VA was also measured with their habitual soft contact lens correction. If the myopic subjects did not reach a monocular Snellen VA of 6/7.5 (20/25) with their own lenses, they were provided with spherical daily disposable soft contact lenses with the spherical equivalent for performing the trial. Accommodation amplitude was measured by taking the mean of three readings using the push-up method. The accommodation response behavior was recorded via a custom-built eccentric infrared photorefractor (Choi et al., 2000; Gekeler, Schaeffel, Howland, & Wattam-Bell, 1997), which was individually calibrated during the first visit using trial lenses and streak retinoscopy (Seidemann & Schaeffel, 2003). Accommodation measurements were taken in the vertical meridian with a sampling frequency of 80 Hz. In the following, only the right eye's accommodation response was analyzed.

On a second visit, the individual accommodation dynamics as well as the ciliary muscle morphology of the right eye were assessed for three different accommodation demands. Myopic subjects were corrected binocularly with soft contact lenses during the entire investigation. First, the closed-loop accommodation behavior for a stimulus step change of far-near-far was recorded via eccentric infrared photorefractor for the dioptric target distances 2.5 D, 3 D, and 4 D. Monocular viewing conditions were created by placing an infrared-transmitting filter (RG695, SCHOTT AG, Mainz, Germany) in front of the subject's left eye. This approach still allowed binocular accommodation response readings via the photorefractor. A display for far target presentation was positioned at 4 m (Diagnosys LLC, Lowell, USA, luminance 50 cd/m<sup>2</sup>, resolution 1920 × 1080 pixels), and a semi-transparent mirror rotated by 45° was placed just in front of the subjects, allowing the simultaneous viewing of the high-resolution near display (Adafruit Qualia 9.7" DisplayPort Monitor, Adafruit, New York City, USA, luminance 2 cd/m<sup>2</sup>) which was positioned to the left front of the subjects. Its position could be individually adjusted for the different accommodation demands by movement on an optical track. Before starting the step pulse, near and far targets were individually aligned in order to avoid gaze shifts during their switch. The fixation stimuli, 5-letter words with a colored central letter and a letter size equivalent to a Snellen VA of 6/12 (20/40), were presented according to the rapid serial visual presentation paradigm and changed with a frequency of 2 Hz, keeping a constant position on the display. They were first shown at the far display, then at the near display at either 40 cm, 33 cm, or 25 cm distance, and then back at the far display for 15 s, respectively, during which the subjects were asked to fixate the colored central letter. For each of the three near target distances, three step pulse measurements were recorded. The order of the distances was randomized. Subsequently, subjects were given a break of 15 min during which they were shown a documentary on a display at 4 m distance to relax their eyes. After the break, the participants sat down in front of an anterior segment OCT (*Visante*, Carl Zeiss Meditec AG, Jena, Germany) and were positioned on the left-sided rest of the instrument. The temporal ciliary muscle of the right eye was imaged with the head positioned parallel to the device and the gaze shifted by 40°, while target fixation was performed by the left eye. A high-resolution display (Adafruit Qualia 9.7" DisplayPort Monitor, luminance 2 cd/m<sup>2</sup>) with an attached semi-transparent mirror was positioned externally at an angle of 40° in front of the subjects. This facilitated the simultaneous view of the reflection of the far target which was presented on a second display at 4 m distance behind the subjects (LG Electronics Deutschland GmbH, Eschborn, Germany; 23.8", resolution 1920 × 1080 pixels). Instrument settings were the same as described previously (Wagner, Zrenner, & Strasser, 2018). Prior to the imaging, an individual target alignment was undertaken to prevent the subjects from moving during the imaging period. Fixation targets were again 5-letter words with a VA demand of Snellen 6/15 (20/50) which changed by 2 Hz, keeping the same position on the display. Subjects were asked to first look at the reflection of the far display and fixate the colored letter. After having taken a minimum of three OCT images, the target was switched to the

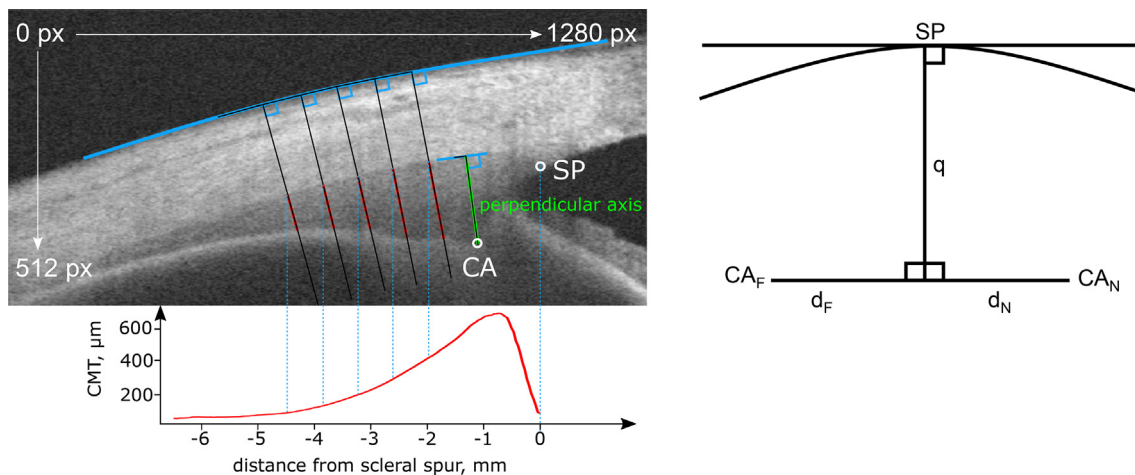


**Fig. 1.** Determination of anatomical measures in OCT images. Left: Definition of CMT profile (red curve) and selective CMT reading, the so-called perpendicular axis ( $CMT_{PA}$ , green line). Right: Calculation of ciliary muscle apex' (CA) shift against position of scleral spur (SP) during far ( $d_F$ ) and near vision ( $d_N$ ). Adapted with permission from (Wagner et al., 2018), OSA. (For interpretation of the references to colour in this figure legend, the reader is referred to the web version of this article.)

near display in front of the subjects. Again, at least three images of the right ciliary muscle were recorded while the subjects fixated the near target. This measurement procedure was performed in random order at all three near target distances (40 cm, 33 cm, and 25 cm), resulting in a minimum of 18 OCT images per subject. Short breaks were given to the subjects between the three imaging sessions. The accommodation response of the left eye was simultaneously monitored using eccentric infrared photorefraction.

### 2.3. Data processing

Accommodation dynamics measurements were filtered for blink artefacts using a custom-written script in JMP (SAS Institute GmbH, Heidelberg, Germany). The mean accommodation dynamics recordings for each subject and distance were fitted using a non-linear model facilitating the calculation of upper and lower asymptotes and accommodation and disaccommodation velocity. OCT images were semi-automatically processed in a masked way via a custom-developed software, resulting in CMT profiles as well as a selective CMT reading perpendicular to the upper muscle border and crossing the muscle's apex (referred to as perpendicular axis,  $CMT_{PA}$ , Fig. 1), and it provided the coordinates of the scleral spur and the ciliary muscle apex (Wagner et al., 2018).

### 2.4. Statistical analysis

The statistical analysis was performed using SPSS Statistics 24 (IBM Deutschland GmbH, Ehningen, Germany) and JMP 14 (SAS Institute GmbH, Heidelberg, Germany). Repeated measures ANOVA with the within-subject factor target distance and the between-subject factor refractive state was applied. Due to its robustness to violations of normality (Blanca, Alarcón, Arnau, Bono, & Bendayan, 2017), an ANOVA was also performed in cases of moderate deviations from normal distribution. Greenhouse-Geisser adjustment was used to correct for violations of sphericity. As OCT images during far vision were taken prior to each near distance condition, the average of the three far vision  $CMT_{PA}$  readings was taken for the analysis of the absolute  $CMT_{PA}$  values. Relationships between CMT and accommodation characteristics were assessed using the Pearson Product Moment correlation coefficient. A linear mixed model with the factors refractive state, target distance,  $CMT_{PA}$  change from far to near vision,  $CMT_{PA}$  during far accommodation and far to near lens changes, and the subject as random factor nested with the refractive state was used to analyze the origin of

the accommodation microfluctuations.

## 3. Results

### 3.1. Subjects characteristics

Mean and SD of the right eye's refractive error in the spherical equivalent was  $0.03 \pm 0.30$  D in the emmetropic and  $-2.44 \pm 1.04$  D in the myopic group. Amplitude of accommodation of the right eye was according to age (emmetropes:  $10.99 \pm 1.80$  D; myopes:  $11.72 \pm 2.22$  D) and all subjects achieved a best-corrected monocular Snellen VA of 6/6 (20/20) or better. A monocular Snellen VA of 6/7.5 (20/25) or better was achieved by uncorrected emmetropic and contact lens-corrected myopic subjects.

### 3.2. Ciliary muscle morphology

#### 3.2.1. Comparison of emmetropic and myopic CMT profiles

The averaged CMT profiles of emmetropic and myopic participants for the different target distances are illustrated in Fig. 2. The origin of the coordinate system is set to the position of the scleral spur and the CMT readings on the ordinate are given in  $\mu\text{m}$ . On the left side, the CMT profile during far vision is plotted, while the right side shows the CMT profile when subjects had adjusted their accommodation response to the near target of either 2.5 D, 3 D, or 4 D (from top to bottom).

The plots demonstrate substantial differences in the shape of the CMT profiles between the two refractive groups: During far vision (Fig. 2 left), the ciliary muscle of emmetropes was thicker than that of myopes in the region from 0 to about 1.4 mm from the scleral spur, while the myopic ciliary muscle was clearly thicker in the subsequent region until about 4.5 mm posterior to the scleral spur. From here, the profiles of the two groups were essentially identical. During near vision (Fig. 2 right), the intersection of the myopic and the emmetropic CMT profile moved anteriorly and was positioned closer to the scleral spur the higher the accommodation demand: For the 2.5 D and 3 D distance, the emmetropic muscle was thicker than the myopic from 0 until 1.35 mm posterior to the scleral spur, and from 0 until 1.25 mm at the 4 D distance. The CMT differences in the area posterior to the profiles' intersection were less during near than during far vision. Fig. 2 markedly illustrates that maximal CMT readings can be found in emmetropic eyes at all tested accommodation demands. While the emmetropic CMT profile exhibits a vertically stretched shape, the myopic CMT profile rather shows a wide, compressed shape, being stretched in the anterior-

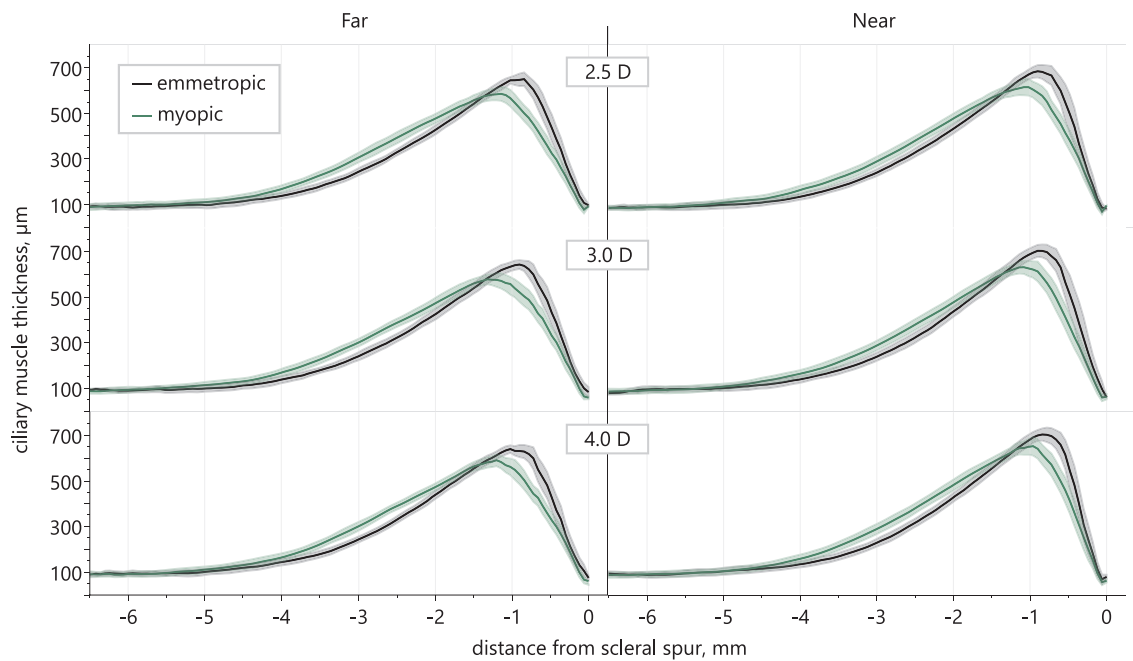


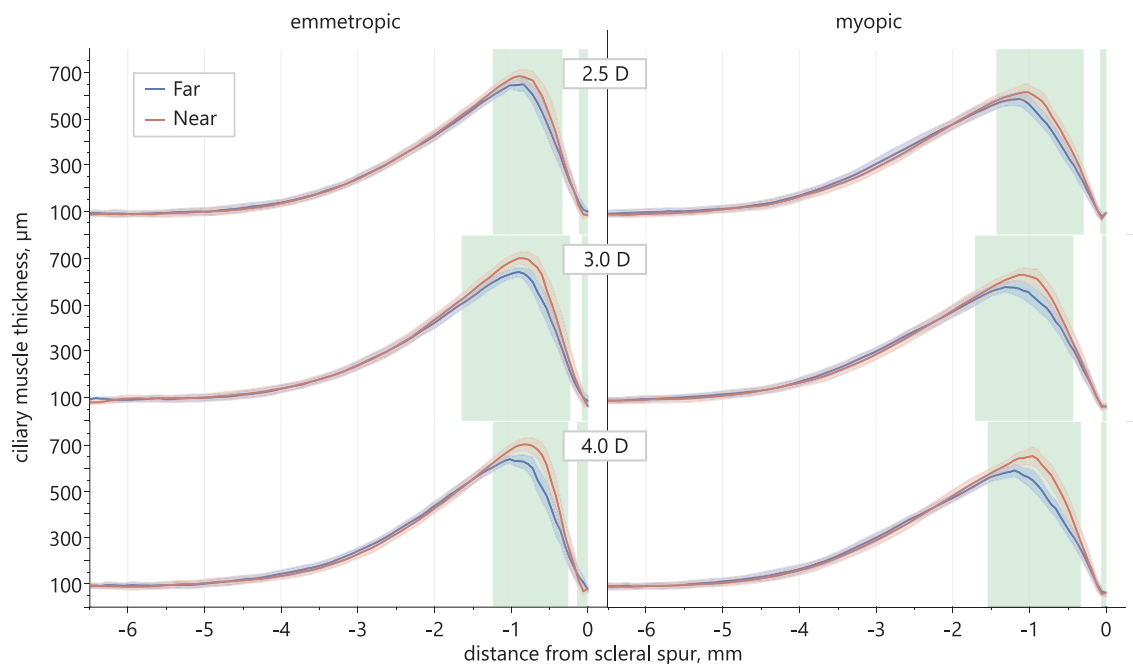
**Fig. 2.** Averaged CMT profiles of emmetropes and myopes. Averaged CMT profiles of 18 emmetropic (black) and 20 myopic subjects (green) for far (left) and near accommodation (right) at the target distances 2.5 D, 3 D, and 4 D (from top to bottom). Far vision measurements were taken before each of the near vision measurements, respectively. Shaded areas denote  $\pm 1$  SD. (For interpretation of the references to colour in this figure legend, the reader is referred to the web version of this article.)

to-posterior direction.

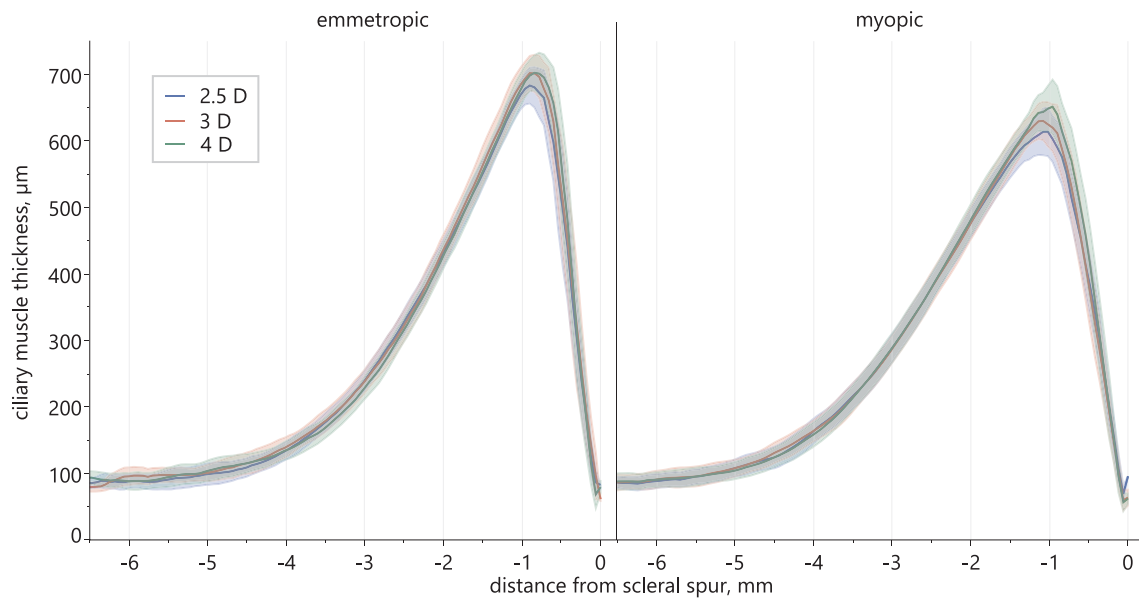
**3.2.2. Comparison of CMT profile changes during accommodation**

Fig. 3 depicts the CMT changes of emmetropic and myopic eyes when accommodating for the three different target distances. For both refractive groups, the main thickness changes occurred in the region up to maximal 2 mm posterior to the scleral spur. From there, the profiles for near and far accommodation were overlaid at all distances in both groups. The areas of the largest thickness changes are highlighted by

green bars. All six far-near CMT profile combinations reveal two areas of largest change: a narrow region of thinning very close to the scleral spur and a wider region of thickening around 1 mm posterior to the scleral spur. Comparing the profiles of emmetropic and myopic participants shows that the latter exhibited a narrower region of thinning. In both refractive groups, the areas of largest change were relatively similar for 2.5 D and 4 D accommodation demand, respectively, however for the target distance of 3 D, the region of thickening became wider, especially in emmetropic eyes.



**Fig. 3.** Averaged CMT profiles during far vs. near accommodation. Averaged CMT profiles for far (blue) and near accommodation (red) for 2.5 D, 3 D, and 4 D accommodation demand (from top to bottom), separately for emmetropic (left) and myopic eyes (right). Shaded areas denote  $\pm 1$  SD. Green bars indicate the regions of the largest thickness changes. (For interpretation of the references to colour in this figure legend, the reader is referred to the web version of this article.)



**Fig. 4.** Averaged CMT profiles for all near distances. Averaged CMT profiles for accommodation by 2.5 D (blue), 3 D (red), and 4 D (green) for emmetropic (left) and myopic eyes (right). Shaded areas represent  $\pm 1$  SD. (For interpretation of the references to colour in this figure legend, the reader is referred to the web version of this article.)

Combining the CMT profiles for the three near target distances in one graph (Fig. 4) shows that myopic eyes changed the shape of their ciliary muscle with increasing accommodation demand, while emmetropic ciliary muscles only revealed shape changes for the step from 2.5 D to 3 D accommodation demand, but not from 3 D to 4 D: The CMT profiles for the target distances 3 D and 4 D were superimposed. The regions where the profile changes between the distances were more anterior in emmetropic eyes than in myopic eyes.

### 3.2.3. Selective CMT readings

Table 1 shows the relative values of  $CMT_{PA}$  for a change of accommodation by 2.5 D, 3 D, and 4 D, respectively. While the  $CMT_{PA}$  of myopic subjects on average exhibited an increase in thickness change

with increasing accommodation demand, emmetropic  $CMT_{PA}$  only revealed an increase from 2.5 D to 3 D, and not from 3 D to 4 D; here, the change decreased. In general, the relative change of  $CMT_{PA}$  when accommodating was less in myopic ciliary muscles than in emmetropic at all three dioptric distances, however without being statistically significant ( $F_{1,36} = 0.999$ ,  $p = 0.324$ ). For 4 D of accommodation demand, the average relative values of the two refractive groups only differed by about 2  $\mu m$ . In both groups, the thickness change from 2.5 D to 3 D was largest with about 27  $\mu m$  difference in emmetropes and 21  $\mu m$  in myopes.

The change of  $CMT_{PA}$  from far to near vision was influenced by the target distance ( $F_{2,72} = 9.196$ ,  $p < 0.001$ ) with significant differences between the distances 2.5 D and 3 D (Bonferroni,  $p = 0.002$ ), as well as

**Table 1**

Relative values of  $CMT_{PA}$ . Changes in  $CMT_{PA}$  ( $\Delta_{far-near}$ ) in the two refractive groups when accommodating by 2.5 D, 3 D, and 4 D.

Emmetropic group (n = 18)				Myopic group (n = 20)			
Subject	$CMT_{PA} \Delta_{far-near}, \mu m$			Subject	$CMT_{PA} \Delta_{far-near}, \mu m$		
	2.5D	3D	4D		2.5D	3D	4D
E1	-45.57	-59.38	-51.82	M1	51.50	-25.07	-86.85
E2	-119.99	-123.96	-85.61	M2	-63.80	-32.49	-96.03
E3	51.56	-15.36	-60.68	M3	-51.56	-79.17	-77.34
E4	-29.69	-97.40	-61.07	M4	-39.00	-84.90	-64.26
E5	-66.41	-72.59	-89.00	M5	-43.03	15.82	-69.53
E6	-90.47	-119.92	-79.17	M6	-68.49	-90.30	-119.53
E7	-4.43	-34.64	-55.98	M7	-21.09	-67.12	-118.88
E8	-33.85	-90.76	-89.97	M8	-32.03	-83.79	-81.64
E9	-29.95	-74.48	-30.73	M9	-23.96	-13.33	-38.22
E10	-78.91	-96.61	-36.98	M10	3.91	-41.34	-69.60
E11	-54.69	-101.04	-56.77	M11	-34.64	-9.05	-5.14
E12	-34.90	-112.76	-99.22	M12	-59.90	-101.82	-61.46
E13	-100.26	-92.58	-73.24	M13	-24.61	-18.23	-6.05
E14	-58.59	-25.39	-73.96	M14	-20.31	2.21	-11.85
E15	-62.24	-42.71	-95.83	M15	-29.88	-80.99	-49.61
E16	-31.25	-16.67	-90.63	M16	-32.23	-18.36	-89.58
E17	26.69	-69.01	-1.04	M17	6.77	-7.03	-25.39
E18	-14.58	-20.25	-55.66	M18	-52.92	-142.90	-21.29
				M19	-92.97	-87.50	-78.39
				M20	-48.76	-125.33	-108.01
<b>mean</b>	<b>-43.20</b>	<b>-70.31</b>	<b>-65.96</b>		<b>-33.85</b>	<b>-54.53</b>	<b>-63.93</b>
<b>SD</b>	<b>42.55</b>	<b>36.80</b>	<b>25.70</b>		<b>30.94</b>	<b>45.31</b>	<b>36.08</b>

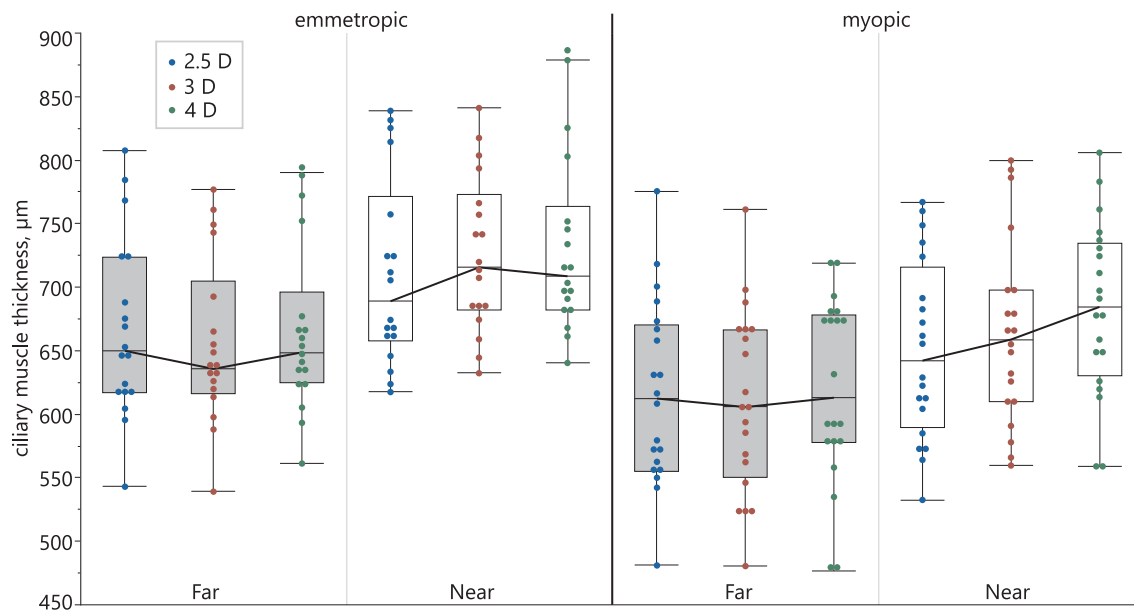


**Fig. 5.** Absolute values of CMT<sub>PA</sub>. Boxplots of the absolute values of CMT<sub>PA</sub> of emmetropic and myopic eyes during far (gray boxes) and near accommodation (white boxes) of 2.5 D (blue points), 3 D (red points), and 4 D (green points). OCT imaging during far vision took place prior to each of the near vision conditions. The black line links the median values of each box. Each point represents the measurement of a subject. (For interpretation of the references to colour in this figure legend, the reader is referred to the web version of this article.)

between 2.5 D and 4 D (Bonferroni,  $p = 0.001$ ). In the myopic group, the change of CMT<sub>PA</sub> from far to near accommodation showed a small, but statistically significant linear relationship with the accommodation demand (Pearson  $R = -0.296$ ,  $p = 0.022$ , two-tailed).

The absolute values of the CMT<sub>PA</sub> in emmetropic and myopic ciliary muscles are shown in Fig. 5. An analysis of the three far vision CMT<sub>PA</sub> readings (gray boxes) revealed a good measurement repeatability (ICC 0.965, 95% confidence interval 0.940 to 0.981). The boxplots for near accommodation (white boxes) show a continuous increase of the CMT<sub>PA</sub> with increasing accommodation demand in myopes while emmetropes did not exhibit an increase in their CMT<sub>PA</sub> for the step from 3 D to 4 D. Moreover, myopic eyes display lower CMT<sub>PA</sub> at all target distances ( $F_{1,36} = 6.458$ ,  $p = 0.015$ ; Table 2). The CMT<sub>PA</sub> was significantly influenced by the accommodation demand ( $F_{3,108} = 55.115$ ,  $p < 0.001$ ).

No significant interaction of refraction and target distance was found ( $F_{3,108} = 0.841$ ,  $p = 0.474$ ).

### 3.2.4. Movement of ciliary muscle during accommodation

As previously described (Wagner et al., 2018), the shift of the ciliary muscle apex relative to the scleral spur during far and near vision can be used to analyze the ciliary muscle’s movement during the process of accommodation. At the 2.5 D distance, the apex was positioned at  $-0.58 \pm 0.13$  mm posterior to the scleral spur during far and at  $-0.46 \pm 0.10$  mm during near vision in emmetropic eyes, and at  $-0.81 \pm 0.18$  mm during far vs.  $-0.70 \pm 0.18$  mm during near vision in myopic eyes. The higher the accommodation demand, the closer the apex moved in a horizontal direction towards the scleral spur, with a larger step from 3 D to 4 D than from 2.5 D to 3 D. Not only was the

**Table 2**

Overview of biometric and accommodative data. Biometric and accommodative data of right eyes of emmetropic and myopic study group (mean  $\pm$  SD). SP = scleral spur; CA = ciliary muscle apex.

	Emmetropic group (n = 18)	Myopic group (n = 20)
CMT <sub>PA</sub> $\Delta_{far-near}$ 2.5D ( $\mu$ m)	$-43.20 \pm 42.55$	$-33.85 \pm 30.94$
CMT <sub>PA</sub> $\Delta_{far-near}$ 3D ( $\mu$ m)	$-70.31 \pm 36.80$	$-54.53 \pm 45.31$
CMT <sub>PA</sub> $\Delta_{far-near}$ 4D ( $\mu$ m)	$-65.96 \pm 25.70$	$-63.93 \pm 36.08$
CMT <sub>PA</sub> 0D ( $\mu$ m)	$662.96 \pm 65.08$	$615.01 \pm 70.52$
CMT <sub>PA</sub> 2.5D ( $\mu$ m)	$710.13 \pm 74.21$	$650.23 \pm 70.74$
CMT <sub>PA</sub> 3D ( $\mu$ m)	$725.93 \pm 61.05$	$663.86 \pm 73.26$
CMT <sub>PA</sub> 4D ( $\mu$ m)	$731.93 \pm 71.85$	$683.20 \pm 68.39$
distance SP-CA $\Delta_{far-near}$ 2.5D (mm)	$0.06 \pm 0.11$	$0.07 \pm 0.07$
distance SP-CA $\Delta_{far-near}$ 3D (mm)	$0.04 \pm 0.09$	$0.11 \pm 0.18$
distance SP-CA $\Delta_{far-near}$ 4D (mm)	$0.09 \pm 0.09$	$0.16 \pm 0.13$
first upper asymptote 2.5D (D)	$-0.96 \pm 0.25$	$-0.77 \pm 0.30$
first upper asymptote 3D (D)	$-0.91 \pm 0.27$	$-0.77 \pm 0.33$
first upper asymptote 4D (D)	$-0.94 \pm 0.31$	$-0.79 \pm 0.27$
second upper asymptote 2.5D (D)	$-0.98 \pm 0.32$	$-0.82 \pm 0.32$
second upper asymptote 3D (D)	$-0.96 \pm 0.31$	$-0.80 \pm 0.32$
second upper asymptote 4D (D)	$-0.96 \pm 0.35$	$-0.85 \pm 0.29$
lag of accommodation 2.5D (D)	$-0.15 \pm 0.41$	$-0.19 \pm 0.36$
lag of accommodation 3D (D)	$-0.29 \pm 0.51$	$-0.43 \pm 0.28$
lag of accommodation 4D (D)	$-0.79 \pm 0.63$	$-0.93 \pm 0.38$
microfluctuations of accommodation 2.5D (D)	$0.38 \pm 0.08$	$0.40 \pm 0.09$
microfluctuations of accommodation 3D (D)	$0.46 \pm 0.11$	$0.48 \pm 0.10$
microfluctuations of accommodation 4D (D)	$0.63 \pm 0.11$	$0.59 \pm 0.10$

position of the ciliary muscle apex more posterior to the scleral spur at all distances in myopic eyes, the ciliary muscle movement for accommodation of 3 D and 4 D ( $\Delta_{\text{far-near}}$ ) was also larger in myopes than in emmetropes (3 D: emmetropes: far  $-0.58 \pm 0.11$  mm, near  $-0.44 \pm 0.13$  mm; myopes: far  $-0.85 \pm 0.21$  mm, near  $-0.68 \pm 0.15$  mm; 4 D: emmetropes: far  $-0.59 \pm 0.15$  mm, near  $-0.39 \pm 0.11$  mm; myopes: far  $-0.85 \pm 0.17$  mm, near  $-0.61 \pm 0.18$  mm).

### 3.2.5. Change of distance between scleral spur and ciliary muscle apex

The Euclidean distance between the coordinates of scleral spur and ciliary muscle apex provides evidence for shape changes of the ciliary muscle due to accommodation. The refractive state of the subjects had a significant influence on the change of the Euclidean distance (Table 2) from far to near accommodation ( $F_{1,36} = 5.013$ ,  $p = 0.031$ ), but not the target distance ( $F_{2,72} = 2.865$ ,  $p = 0.063$ ), nor their interaction ( $F_{2,72} = 0.981$ ,  $p = 0.380$ ). Both the absolute values of the distance between scleral spur and ciliary muscle apex, as well as the changes from far to near vision, were larger in myopic than in emmetropic eyes at all three dioptric distances. In both refractive groups, the distance between these two landmarks decreased during near accommodation, with the largest decrease at 4 D. Interestingly, while this relative change from far to near vision continuously increased with increasing accommodation demand in myopes (Pearson  $R = 0.273$ ,  $p = 0.035$ , two-tailed), such a continuous change was not found in emmetropes (Pearson  $R = 0.153$ ,  $p = 0.269$ , two-tailed).

## 3.3. Accommodation dynamics

### 3.3.1. Accommodation response for far and near target period

The non-linear model for fitting the accommodation response resulted in the values for the asymptotes of the first far vision period ( $u_1$ ), the near period ( $b$ ) and the second far vision period ( $u_2$ ), and the first derivative provided the velocity of accommodation and disaccommodation. Both the first and the second upper asymptote were lower in the myopic group, however without reaching statistical significance ( $u_1$ :  $F_{1,36} = 3.112$ ,  $p = 0.086$ ;  $u_2$ :  $F_{1,36} = 2.000$ ,  $p = 0.166$ ; Table 2). The velocity of accommodation and disaccommodation did not differ between emmetropes and myopes (accommodation:  $F_{1,36} = 0.460$ ,  $p = 0.502$ ; disaccommodation:  $F_{1,35} = 0.375$ ,  $p = 0.544$ ). The analysis of the lower asymptote revealed increasing lags of accommodation for closer target distances ( $F_{1,62,58,39} = 202.708$ ,  $p < 0.001$ ), without a significant influence of refractive state ( $F_{1,36} = 0.622$ ,  $p = 0.436$ ; Table 2).

Analyzing the difference between the asymptotes of the first far and the near period ( $\Delta_{u_1-b}$ ), as well as of the near and the second far period ( $\Delta_{b-u_2}$ ), demonstrated that the two refractive groups did not significantly differ in their accommodation change from far to near vision ( $F_{1,36} = 0.219$ ,  $p = 0.643$ ), or from near to far vision ( $F_{1,36} = 0.092$ ,  $p = 0.763$ ).

### 3.3.2. Microfluctuations of accommodation

Accommodation variability in the two study groups was determined from the standard deviations of the accommodation responses (Harb et al., 2006) at each of the three distances. The individual calibration of the photorefractor, reducing measurement errors to 0.25 D or less (Gekeler et al., 1997), and the sampling rate of 80 Hz allowed for the detection of accommodation microfluctuations (Campbell, Robson, & Westheimer, 1959; Charman & Heron, 1988). The microfluctuations (Table 2) significantly increased with increasing accommodation demand ( $F_{2,72} = 162.163$ ,  $p < 0.001$ ) and there was a significant interaction effect between accommodation demand and refractive state ( $F_{2,72} = 3.768$ ,  $p = 0.028$ ). However, the refractive state did not show a significant main effect on the amount of microfluctuation ( $F_{1,36} = 0.003$ ,  $p = 0.955$ ).

### 3.3.3. Power spectrum analysis

Power spectrum analysis was performed using the Lomb-Scargle periodogram. The sum of the power spectral density (sum(psd)) of low (LFC, 0.1–0.6 Hz), medium (MFC, 0.6–1 Hz), and high frequency components (HFC, 1–2.3 Hz) was calculated for the near vision period for each group and distance. To account for large deviations from normality, the logarithm of sum(psd) was used to perform repeated measures ANOVAs, revealing a significant influence of accommodation demand in all three frequency components (LFC:  $F_{2,72} = 82.888$ ; MFC:  $F_{2,72} = 46.218$ ; HFC:  $F_{2,72} = 37.743$ ,  $p < 0.001$ , respectively), while the refractive state did not affect the sum(psd) (LFC:  $F_{1,36} = 1.743$ ,  $p = 0.195$ ; MFC:  $F_{1,36} = 0.038$ ,  $p = 0.847$ ; HFC:  $F_{1,36} = 0.111$ ,  $p = 0.741$ ).

## 3.4. Correlation between morphologic and refractive changes

The subjects' spherical equivalent was significantly correlated with the selective CMT reading ( $\text{CMT}_{\text{PA}}$ ) during 2.5 D (Pearson  $R = 0.458$ ,  $p = 0.004$ ), 3 D (Pearson  $R = 0.475$ ,  $p = 0.003$ ), and 4 D accommodation demand (Pearson  $R = 0.403$ ,  $p = 0.012$ ), demonstrating thicker  $\text{CMT}_{\text{PA}}$  in less myopic eyes. The  $\text{CMT}_{\text{PA}}$  readings were analyzed in relation to the accommodation response behavior of the subjects' right eyes during the step pulse (Table 2). For the stimulus level 4 D, a larger  $\text{CMT}_{\text{PA}}$  was linked with larger microfluctuations during the near vision phase of the step change (Pearson  $R = 0.430$ ,  $p = 0.007$ ). Larger changes of the  $\text{CMT}_{\text{PA}}$  ( $\text{CMT}_{\text{PA}} \Delta_{\text{far-near}}$ ) for a 4 D demand were associated with lower accommodation response changes during disaccommodation in the 0 D - 4 D - 0 D step pulse ( $\Delta_{b-u_2}$ , Pearson  $R = -0.381$ ,  $p = 0.018$ ). Analyzing the two refractive groups separately revealed no significant correlation between the accommodation-induced changes of  $\text{CMT}_{\text{PA}}$  and the accommodation response changes in the step pulse in emmetropes. However, in myopes, for an accommodation demand of 4 D, larger  $\text{CMT}_{\text{PA}}$  changes were significantly correlated with lower accommodation response changes from far to near (Pearson  $R = 0.533$ ,  $p = 0.015$ ) and from near to far vision (Pearson  $R = -0.578$ ,  $p = 0.008$ ). The larger the change of the  $\text{CMT}_{\text{PA}}$  in a myopic subject for an accommodation demand of 4 D, the higher the lag of accommodation in the step pulse at the same distance (Pearson  $R = 0.449$ ,  $p = 0.047$ ).

The linear mixed model demonstrated that the accommodation microfluctuations can primarily be explained by the refractive power changes of the lens when adjusting for near vision ( $p < 0.001$ ) as well as by the  $\text{CMT}_{\text{PA}}$  changes as a function of accommodation demand ( $p = 0.012$ ). The  $\text{CMT}_{\text{PA}}$  during far accommodation also influenced the amount of microfluctuation, but not significantly ( $p = 0.078$ ). No significant effect of refractive state was revealed ( $p = 0.986$ ).

## 4. Discussion

The accommodation behavior as well as the morphology of the ciliary muscle were previously found to depend on the refractive state of the subjects. The current analysis confirms these findings with respect to the ciliary muscle, demonstrating significant differences between emmetropic and myopic eyes in the muscle shape, thickness, and movement of ciliary muscle apex in relation to scleral spur. The accommodation response behavior to a step change of the pattern far-near-far however only revealed minor differences between the two study groups.

### 4.1. Substantial differences in ciliary muscle morphology of emmetropic and myopic eyes

To the best of our knowledge, this is the first investigation comparing the ciliary muscle shape changes across the entire muscle boundary for different accommodation demands in emmetropic and myopic eyes. Moreover, this is also the first time that ciliary muscle

shape changes are analyzed in relation to the accommodation dynamics. To date, only selective or proportional CMT readings were taken for various accommodation stimuli resulting in rather diverging values (Lossing et al., 2012; Richdale et al., 2012; Shao et al., 2013; Sheppard & Davies, 2010). Different outcomes might not only derive from the measurement device and procedure and the examined study population, but also from the process of ciliary muscle segmentation and the definition of its boundaries and of the scleral spur position. So far, no completely objective segmentation tool for ciliary muscle analysis is available that could prevent an examiner's bias in defining the muscle's thickness. In addition, the selective thickness readings only give a narrow insight into the muscle morphology and impede the evaluation of the entire muscle's behavior during accommodation. By providing a continuous thickness measurement across the boundaries of the ciliary muscle during far and near accommodation, the presented methodology provides a powerful tool for ciliary muscle analysis which overcomes the disadvantages of selective or proportional readings. The CMT profiles presented here reveal an anterior thinning and a posterior thickening of the ciliary muscle during accommodation, whereby the thinning area was found to be narrower in myopic than in emmetropic eyes. A posterior muscle thinning in the area 2 to 3 mm from the scleral spur as reported in previous trials (Lewis et al., 2012; Lossing et al., 2012; Richdale et al., 2013; Sheppard & Davies, 2010) could not be confirmed. Shape changes between the two study groups were present during far and near vision with thicker emmetropic muscles until about 1.4 mm posterior to the scleral spur and subsequent thicker myopic ciliary muscles. Moreover, the ciliary muscle in myopic eyes, contrary to emmetropic eyes, increased its relative thickness from far to near vision for each increase in accommodation demand. Similar to our finding of larger thickness changes from 2.5 D to 3 D than from 3 D to 4 D, Sheppard and Davies also observed greater changes of both CMT and ciliary muscle length for a step change from 0.19 to 4 D than from 4 to 8 D (Sheppard & Davies, 2010). It is possible that this difference reflects the previous finding of increasing accommodative lags with larger demands of accommodation (Bullimore, Gilmartin, & Royston, 1992; Nakatsuka et al., 2005; Seidemann & Schaeffel, 2003).

In the current trial, the  $CMT_{PA}$  increase during accommodation was lower in myopic than in emmetropic eyes at 2.5 D and 3 D, and only at 4 D was the increase essentially equal in both refractive groups. Moreover, the absolute  $CMT_{PA}$  readings were significantly smaller in the myopic participants. The ciliary muscle apex was positioned more posteriorly in the myopic group and revealed a larger shift for accommodation of 3 D and 4 D than in emmetropic eyes. Both the changes of the ciliary muscle apex position relative to the scleral spur, as well as the changes of the distance between these two landmarks during accommodation, provide evidence for a larger ciliary muscle movement in myopic than in emmetropic eyes, thereby contradicting previous findings (Jeon et al., 2012). Additionally, with respect to muscle shape changes, the distance changes between scleral spur and ciliary muscle apex when changing accommodation from far to near vision continuously increased with increasing accommodation demand in myopes, but not in emmetropes.

#### 4.2. Minor differences in accommodation dynamics

The accommodation dynamics analysis revealed, in contrast to published data (Harb et al., 2006; Langaas et al., 2008), that microfluctuations of myopic accommodation near responses were not increased compared to those of emmetropes. Neither did the power spectral density of the accommodation significantly differ between the two study groups, nor the relative change of the lens power for adjustment from far to near vision and vice versa at the three target distances, nor the velocity of the change. A dependence between refractive error and the speed of accommodation or near to far accommodation was also not found by Schaeffel, Wilhelm, and Zrenner (1993). It is possible that the short measurement period (in contrast to Harb et al.,

2006) and the subjects' age (young adults, in contrast to Langaas et al., 2008) of the current trial prevented the finding of increased microfluctuations in myopic participants.

As shown before (Gwiazda et al., 1993), myopic subjects exhibited slightly larger lags of accommodation for all tested accommodation demands, however without reaching statistical significance.

#### 4.3. Relationship between morphologic ciliary muscle and crystalline lens changes

Previous investigations found evidence for a linear relationship between the CMT during accommodation and the accommodation response (Lewis et al., 2012; Richdale et al., 2013). A thickening of the anterior and a thinning of the posterior muscle portion with increasing accommodation response, either taken via photorefractometry during OCT imaging (Lewis et al., 2012) or via autorefractometry prior to the imaging (Richdale et al., 2013), was measured. The current study revealed a continuous increase of the anterior CMT changes from far to near vision ( $CMT_{PA} \Delta_{far-near}$ ) with increasing accommodation demand in myopic participants. Lewis and colleagues suggested that subjects aimed to accommodate in a way to keep the ciliary muscle changes in a linear range, which then could lead to a lag of accommodation (Lewis et al., 2012). Evidence for this hypothesis is provided by the current finding of a linear change of  $CMT_{PA}$  with increasing accommodation demand in myopes, in contrast to emmetropes, and the corresponding larger lags of accommodation during the step pulse in the former. Just like the lag of accommodation (Gwiazda et al., 1993), accommodation microfluctuations, when temporally integrated, were previously suggested to be a potential causative factor in myopia development (Harb et al., 2006). Could the ciliary muscle rather than the crystalline lens be the origin of the microfluctuations? We found that – independent of the refractive error – the accommodation variability can be explained to some extent by the  $CMT_{PA}$  changes during accommodation, but a larger impact on the microfluctuations is given by the lens properties. It seems that the dynamics of accommodation are more strongly determined by the biomechanical features of the crystalline lens than the anatomical structure of the ciliary muscle. Further insight into the relationship between CMT and lens changes might be provided by testing higher accommodation demands.

#### 4.4. Ciliary muscle characteristics as a causative factor in myopigenesis?

A possible relationship between ciliary muscle and axial eye growth was first suggested by van Alphen after having found that in vitro inflation of the eye globe led to a stretching of the ciliary muscle and axial elongation without large changes in the choroid (Van Alphen, 1986). Contrary to this theory, Sheppard and Davies suggested that ocular elongation and radial growth in the form of ciliary muscle thickening are concomitant factors in myopigenesis (Sheppard & Davies, 2010). Buckhurst and colleagues found the total ocular volume to be positively correlated with the CMT measurements and hypothesized that anterior and posterior ocular growth are not matched in myopic eyes due to a deficit in feedback between fovea and ciliary muscle (Buckhurst et al., 2013). Bailey et al. suggested that a thicker ciliary muscle as found in their myopic study population could prevent the equatorial ocular growth and thus result in the axial growth (Bailey et al., 2008). In the current analysis, a significant linear correlation between  $CMT_{PA}$  during near accommodation and the refractive error was found with larger thickness readings being associated with more positive spherical equivalents. This contrasts with previous studies, but can be attributed to the position of measurements, which was more posterior to the scleral spur in the other trials (Bailey et al., 2008; Buckhurst et al., 2013). Our findings of a thicker  $CMT_{PA}$  in emmetropic eyes at this anterior measurement location are in agreement with reports investigating an anisometropic (Kuchem et al., 2013) and a pediatric population (Pucker et al., 2013). Fig. 6 shows examples of an

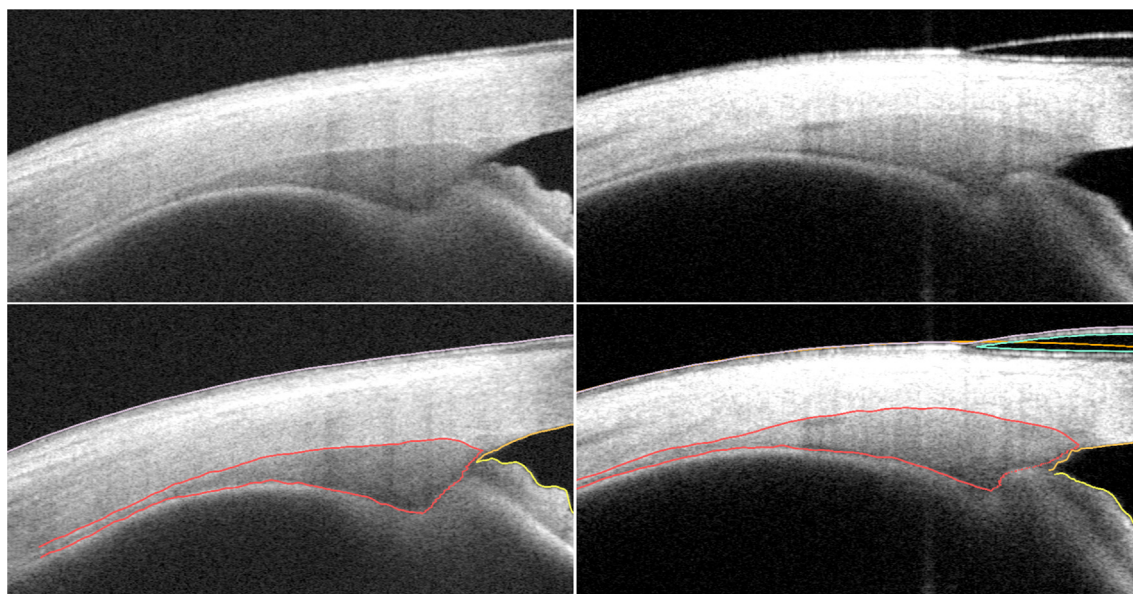


**Fig. 6.** Examples of ciliary muscle of emmetrope and myope. Exemplary OCT images with and without segmentation of an emmetrope (left) and a myopic ciliary muscle (right) during far accommodation.

emmetrope (left) and a myopic ciliary muscle (right) during far vision, clearly illustrating the shape differences in the anterior region between ciliary muscle apex and scleral spur. The question arises why the myopic ciliary muscle is thinner than the emmetrope in the anterior part and only thicker from 1.4 mm posterior to the scleral spur. Could this specific ciliary muscle shape be a precursor or rather the consequence of the prolate form of the myopic eye globe?

In the region close to the scleral spur, the ciliary muscle consists predominantly of longitudinal fibers that have been shown to have less mitochondria and more myofibrils than fibers in the radial portion (Ishikawa, 1962; Tamm & Lütjen-Drecoll, 1996). As these are features of the fast fibers of striated muscles, it was hypothesized that the meridional part of the ciliary muscle can contract faster than the residual muscle parts and provides the stiffness for effective accommodation. In contrast, the circular fibers in the apical muscle region resemble slow tonic type I fibers due to their large amount of mitochondria (Flügel, Bárány, & Lütjen-Drecoll, 1990). Our result of a thinner anterior myopic muscle is in agreement with van Alphen's choroidal expansion model (Van Alphen, 1986) while the larger thickness in the posterior region contradicts it. As found during the scleral thinning in highly myopic eyes (Avetisov, Savitskaya, Vinetskaya, and Iomdina (1983); Summers Rada, Shelton, & Norton, 2006), the thinner anterior part could result from a loss in tissue and changed tissue properties. A thinner apical region with a loss of type I fiber-like circular fibers could result in accommodation inaccuracies during prolonged nearwork tasks. In addition, a thinner longitudinal portion could reduce the stiffness and thus the effectiveness of accommodation, equally leading to the inaccuracies of accommodation of myopic eyes. If this hypothesis holds true, one would expect thinner  $CMT_{PA}$  in eyes with large accommodation microfluctuations, however, the opposite was found at the 4 D distance. Although we did not find a significant relationship between the lag of accommodation and the  $CMT_{PA}$ , it seems plausible that the reduced amount of type I fibers in myopic eyes could be causative for their lower tonic accommodation (Maddock et al., 1981). In two previous trials, ciliary muscle OCT images were analyzed with respect to the muscle's different fiber orientations. By subtracting the CMT readings at 2 mm posterior to the scleral spur from the maximal CMT readings and from those at 1 mm, the muscle's apical region was thought to be isolated. Having found a significantly thicker apical part of the ciliary muscle in more hyperopic eyes, the authors hypothesized that the circular and radial fibers in the

apical region are responsible for the accommodative workload which is increased in hyperopic eyes: Following the muscle-stress response, hyperopes would habitually stress their ciliary muscle, similar to that found during resistance training of a skeletal muscle (Kuchem et al., 2013; Pucker et al., 2013). According to this theory, sustained near vision tasks would also lead to thicker apical ciliary muscles. Both of our study groups, however, consisted of students who were exposed to long periods of nearwork daily, and we find, nevertheless, thicker apical muscles, i.e.  $CMT_{PA}$ , only in the emmetrope participants. Additionally, as OCT imaging does not allow for a discrimination of the different fiber types, it remains unclear which of them is affected by the specific shape alterations. It first needs to be analyzed whether there are differences in the specific fiber composition of the ciliary muscle in eyes of different refractive errors and secondly whether the dimensions of the ciliary muscle's anterior region of non-myopic or that of myopic eyes are the abnormal finding. If the latter was true, it still needs to be investigated whether this anterior muscle thinning is a concomitant process or precedes the development of myopia.

Not only the different CMT profiles were a striking outcome of this investigation. We furthermore found a lower change of  $CMT_{PA}$  with at the same time larger ciliary muscle movement in accommodating myopic eyes compared to emmetrope. Also, smaller changes of  $CMT_{PA}$  are related to larger lens power changes for both accommodation and disaccommodation at the 4 D distance in myopic eyes. Does the increased movement somehow compensate for the lower thickness changes? A larger forward shift of the muscle could lead to a further slackening of the zonules, thereby allowing the lens to perform a larger shape change towards a more convex form. Besides, it remains an open question why only myopes exhibit linear changes regarding  $CMT_{PA}$  and muscle shape and whether this is related to their refractive error development.

Clarification cannot be provided with the current data but requires further investigations including sound histochemical and histological analyses of the ciliary muscle in emmetrope and myopic eyes.

## 5. Conclusion

This is the first study to assess the ciliary muscle thickness changes during accommodation along the entire muscle boundary and to correlate the results with the accommodation dynamics in emmetrope and myopic young adults. Significant differences in ciliary muscle thickness,

shape, and movement were found depending on the refractive error, however, in contrast to previous work, accommodation dynamics were not affected by the refractive state. Remarkable features of the myopic ciliary muscle and its behavior during accommodation were revealed requiring further comparative investigations of the muscle's anatomical shape and histology in non-myopic vs. myopic eyes to assess a possible impact of the ciliary muscle on myopigenesis.

### Declaration of Competing Interest

The authors declare that they have no known competing financial interests or personal relationships that could have appeared to influence the work reported in this paper.

### Acknowledgements

We would like to thank the staff of the workshop of the University Eye Hospital Tuebingen for support in constructing the experimental set-up, the University Eye Hospital Tuebingen and the ZEISS Vision Science Lab at the Institute for Ophthalmic Research in Tuebingen for their proportionate acquisition of the OCT device and the ZEISS Vision Science Lab for providing access to their measuring equipment. We also thank the two unknown reviewers for their constructive comments.

### Funding

Sandra Wagner acknowledges support from the Hector Fellow Academy. Eberhart Zrenner is supported by a grant of the DFG Excellence Program (EXC 307, Centre for Integrative Neuroscience).

### References

- Avetisov, E. S., Savitskaya, N. F., Vinetskaya, M. I., & Iomdina, E. N. (1983). A study of biochemical and biomechanical qualities of normal and myopic eye sclera in humans of different age groups. *Metabolic, Pediatric, and Systemic Ophthalmology*, 7(4), 183–188.
- Bailey, M. D., Sinnott, L. T., & Mutti, D. O. (2008). Ciliary body thickness and refractive error in children. *Investigative Ophthalmology and Visual Science*, 49(10), 4353–4360. <https://doi.org/10.1167/iov.08-2008>.
- Blanca, M., Alarcón, R., Arnau, J., Bono, R., & Bendayan, R. (2017). Non-normal data: Is ANOVA still a valid option? *Psicothema*, 29(4), 552–557. <https://doi.org/10.7334/psicothema2016.383>.
- Buckhurst, H., Gilmartin, B., Cubbidge, R. P., Nagra, M., & Logan, N. S. (2013). Ocular biometric correlates of ciliary muscle thickness in human myopia. *Ophthalmic and Physiological Optics*, 33(3), 294–304. <https://doi.org/10.1111/opo.12039>.
- Bullimore, M. A., Gilmartin, B., & Royston, J. M. (1992). Steady-state accommodation and ocular biometry in late-onset myopia. *Documenta Ophthalmologica*, 80(2), 143–155. <https://doi.org/10.1007/BF00161240>.
- Campbell, F. W., Robson, J. G., & Westheimer, G. (1959). Fluctuations of accommodation under steady viewing conditions. *The Journal of Physiology*, 145(3), 579–594. <https://doi.org/10.1113/jphysiol.1959.sp006164>.
- Charman, W. N., & Heron, G. (1988). Fluctuations in accommodation: A review. *Ophthalmic and Physiological Optics*, 8(2), 153–164. <https://doi.org/10.1111/j.1475-1313.1988.tb01031.x>.
- Choi, M., Weiss, S., Schaeffel, F., Seidemann, A., Howland, H. C., Wilhelm, B., & Wilhelm, H. (2000). Laboratory, clinical, and kindergarten test of a new eccentric infrared photorefractor (PowerRefractor). *Optometry and Vision Science*, 77(10), 537–548. <https://doi.org/10.1097/00006324-200010000-00008>.
- Ciuffreda, K. J., & Vasudevan, B. (2008). Nearwork-induced transient myopia (NITM) and permanent myopia – Is there a link? *Ophthalmic and Physiological Optics*, 28(2), 103–114. <https://doi.org/10.1111/j.1475-1313.2008.00550.x>.
- Ciuffreda, K. J., & Wallis, D. M. (1998). Myopes show increased susceptibility to nearwork aftereffects. *Investigative Ophthalmology and Visual Science*, 39(10), 1797–1803.
- Day, M., Strang, N. C., Seidel, D., Gray, L. S., & Mullen, E. A. H. (2006). Refractive group differences in accommodation microfluctuations with changing accommodation stimulus. *Ophthalmic and Physiological Optics*, 26(1), 88–96. <https://doi.org/10.1111/j.1475-1313.2005.00347.x>.
- Flügel, C., Bárány, E. H., & Lütjen-Drecoll, E. (1990). Histochemical differences within the ciliary muscle and its function in accommodation. *Experimental Eye Research*, 50(2), 219–226. [https://doi.org/10.1016/0014-4835\(90\)90234-L](https://doi.org/10.1016/0014-4835(90)90234-L).
- Gekeler, F., Schaeffel, F., Howland, H. C., & Wattam-Bell, J. (1997). Measurement of astigmatism by automated infrared photoretinoscopy. *Optometry and Vision Science*, 74(7), 472–482.
- Gwiazda, J., Thorn, F., Bauer, J., & Held, R. (1993). Myopic children show insufficient accommodative response to blur. *Investigative Ophthalmology and Visual Science*, 34(3), 690–694.
- Harb, E., Thorn, F., & Troilo, D. (2006). Characteristics of accommodative behavior during sustained reading in emmetropes and myopes. *Vision Research*, 46(16), 2581–2592. <https://doi.org/10.1016/j.visres.2006.02.006>.
- Holden, B. A., Fricke, T. R., Wilson, D. A., Jong, M., Naidoo, K. S., Sankaridurg, P., ... Resnikoff, S. (2016). Global prevalence of myopia and high myopia and temporal trends from 2000 through 2050. *Ophthalmology*, 123(5), 1036–1042. <https://doi.org/10.1016/j.ophtha.2016.01.006>.
- Ishikawa, T. (1962). Fine structure of the human ciliary muscle. *Investigative Ophthalmology*, 1(5), 587–608.
- Jeon, S., Lee, W. K., Lee, K., & Moon, N. J. (2012). Diminished ciliary muscle movement on accommodation in myopia. *Experimental Eye Research*, 105, 9–14. <https://doi.org/10.1016/j.exer.2012.08.014>.
- Kuchem, M. K., Sinnott, L. T., Kao, C.-Y., & Bailey, M. D. (2013). Ciliary muscle thickness in anisometropia. *Optometry and Vision Science*, 90(11), 1312–1320. <https://doi.org/10.1097/OPX.000000000000070>.
- Langaas, T., Riddell, P. M., Svarverud, E., Ystenaes, A. E., Langeeggen, I., & Bruenech, J. R. (2008). Variability of the accommodation response in early onset myopia. *Optometry and Vision Science*, 85(1), 37–48. <https://doi.org/10.1097/OPX.0b013e31815ed6e9>.
- Lewis, H. A., Kao, C. Y., Sinnott, L. T., & Bailey, M. D. (2012). Changes in ciliary muscle thickness during accommodation in children. *Optometry and Vision Science*, 89(5), 727–737. <https://doi.org/10.1097/OPX.0b013e318253de7e>.
- Lossing, L. A., Sinnott, L. T., Richdale, K., & Bailey, M. D. (2012). Measuring changes in ciliary muscle thickness with accommodation in young adults. *Optometry and Vision Science*, 89(5), 719–726. <https://doi.org/10.1097/OPX.0b013e318252eac4>.
- Maddock, R. J., Millodot, M., Leat, S., & Johnson, C. A. (1981). Accommodation responses and refractive error. *Investigative Ophthalmology and Visual Science*, 20(3), 387–391.
- McBrien, N. A., & Millodot, M. (1986). The effect of refractive error on the accommodative response gradient. *Ophthalmic and Physiological Optics*, 6(2), 145–149.
- McBrien, N. A., & Millodot, M. (1987). The relationship between tonic accommodation and refractive error. *Investigative Ophthalmology and Visual Science*, 28(6), 997–1004.
- Morgan, I. G., & Rose, K. A. (2013). Myopia and international educational performance. *Ophthalmic and Physiological Optics*, 33(3), 329–338. <https://doi.org/10.1111/opo.12040>.
- Muftuoglu, O., Hosal, B. M., & Zilelioglu, G. (2009). Ciliary body thickness in unilateral high axial myopia. *Eye*, 23(5), 1176–1181. <https://doi.org/10.1038/eye.2008.178>.
- Mutti, D. O. (2010). Hereditary and environmental contributions to emmetropization and myopia. *Optometry and Vision Science*, 87(4), 255–259.
- Nakatsuka, C., Hasebe, S., Nonaka, F., & Ohtsuki, H. (2005). Accommodative lag under habitual seeing conditions: Comparison between myopic and emmetropic children. *Japanese Journal of Ophthalmology*, 49(3), 189–194. <https://doi.org/10.1007/s10384-004-0175-7>.
- Pucker, A. D., Sinnott, L. T., Kao, C. Y., & Bailey, M. D. (2013). Region-specific relationships between refractive error and ciliary muscle thickness in children. *Investigative Ophthalmology and Visual Science*, 54(7), 4710–4716. <https://doi.org/10.1167/iov.13-11658>.
- Richdale, K., Bailey, M. D., Sinnott, L. T., Kao, C. Y., Zadnik, K., & Bullimore, M. A. (2012). The effect of phenylephrine on the ciliary muscle and accommodation. *Optometry and Vision Science*, 89(10), 1507–1511. <https://doi.org/10.1097/OPX.0b013e318269c8d0>.
- Richdale, K., Sinnott, L. T., Bullimore, M. A., Wassenaar, P. A., Schmalbrock, P., Kao, C. Y., ... Zadnik, K. (2013). Quantification of age-related and per diopter accommodative changes of the lens and ciliary muscle in the emmetropic human eye. *Investigative Ophthalmology and Visual Science*, 54(2), 1095–1105. <https://doi.org/10.1167/iov.12-10619>.
- Ruggeri, M., de Freitas, C., Williams, S., Hernandez, V. M., Cabot, F., Yesilirmak, N., ... Manns, F. (2016). Quantification of the ciliary muscle and crystalline lens interaction during accommodation with synchronous OCT imaging. *Biomedical Optics Express*, 7(4), 1351–1364. <https://doi.org/10.1364/BOE.7.001351>.
- Schaeffel, F., Wilhelm, H., & Zrenner, E. (1993). Inter-individual variability in the dynamics of natural accommodation in humans: Relation to age and refractive errors. *Journal of Physiology*, 461(1), 301–320. <https://doi.org/10.1113/jphysiol.1993.sp019515>.
- Seidemann, A., & Schaeffel, F. (2003). An evaluation of the lag of accommodation using photorefractometry. *Vision Research*, 43(4), 419–430. [https://doi.org/10.1016/S0042-6989\(02\)00571-0](https://doi.org/10.1016/S0042-6989(02)00571-0).
- Shao, Y., Tao, A., Jiang, H., Shen, M., Zhong, J., Lu, F., & Wang, J. (2013). Simultaneous real-time imaging of the ocular anterior segment including the ciliary muscle during accommodation. *Biomedical Optics Express*, 4(3), 466–480. <https://doi.org/10.1364/BOE.4.000466>.
- Sheppard, A. L., & Davies, L. N. (2010). In vivo analysis of ciliary muscle morphologic changes with accommodation and axial ametropia. *Investigative Ophthalmology and Visual Science*, 51(12), 6882–6889. <https://doi.org/10.1167/iov.10-5787>.
- Summers Rada, J. A., Shelton, S., & Norton, T. T. (2006). The sclera and myopia. *Experimental Eye Research*, 82(2), 185–200. <https://doi.org/10.1016/j.exer.2005.08.009>.
- Tamm, E. R., & Lütjen-Drecoll, E. (1996). Ciliary Body. *Microscopy Research and Technique*, 33(5), 390–439.
- Tarrant, J., Severson, H., & Wildsoet, C. F. (2008). Accommodation in emmetropic and myopic young adults wearing bifocal soft contact lenses. *Ophthalmic and Physiological Optics*, 28(1), 62–72. <https://doi.org/10.1111/j.1475-1313.2007.00529.x>.
- Van Alphen, G. W. H. M. (1986). Choroidal stress and emmetropization. *Vision Research*, 26(5), 723–734. [https://doi.org/10.1016/0042-6989\(86\)90086-6](https://doi.org/10.1016/0042-6989(86)90086-6).
- Verhoeven, V. J. M., Buitendijk, G. H. S., Rivadeneira, F., Uitterlinden, A. G., Vingerling, J. R., Hofman, A., & Klaver, C. C. W. (2013). Education influences the role of genetics in myopia. *European Journal of Epidemiology*, 28(12), 973–980. <https://doi.org/10.1007/s10654-013-9856-1>.
- Wagner, S., Zrenner, E., & Strasser, T. (2018). Ciliary muscle thickness profiles derived from optical coherence tomography images. *Biomedical Optics Express*, 9(10), 5100–5114. <https://doi.org/10.1364/BOE.9.005100>.
- Williams, K. M., Bertelsen, G., Cumberland, P., Wolfram, C., Verhoeven, V. J. M., Anastasopoulos, E., ... Hammond, C. J. (2015). Increasing prevalence of myopia in Europe and the impact of education. *Ophthalmology*, 122(7), 1489–1497. <https://doi.org/10.1016/j.ophtha.2015.03.018>.